Temperature dependent relativistic mean field for highly excited hot nuclei

Y. K. Gambhir,[1] J. P. Maharana,[1] G. A. Lalazissis,[2,3] C. P. Panos,[2] and P. Ring[3]
[1]*Department of Physics, Indian Institute of Technology, Bombay, Powai, Mumbai 400 076, India*
[2]*Department of Physics, Aristotle University of Thessaloniki, GR-54006 Thessaloniki, Greece*
[3]*Physics Department, Technical University of Munich, D-85747 Garching, Germany*
(Received 24 July 2000; published 10 October 2000)

The temperature dependent relativistic mean field (RMF-T) results obtained by using nonlinear Lagrangian parameter set NL3 are presented for a few selected representative spherical and deformed nuclei. The calculated total binding energy (entropy) decrease (increase) as temperature (T) increases. The depths of the potentials and the single particle (sp) energies change very little with temperature. The density slightly spreads out; as a result the radius increases as temperature rises. For well deformed nuclei the shell effects disappear at around $T\sim 3$ MeV. This value of T is relatively higher as compared to the corresponding value of T (~ 1.8 MeV) obtained in the Strutinsky-type calculations. This difference in the value of T is shown to be due to the use of the effective nucleon mass ($<$ the bare mass) appearing in the Skyrme III interaction or emerging from the RMF Lagrangian.

PACS number(s): 21.10.Ft, 21.60.Jz, 21.90.+f

I. INTRODUCTION

The study of hot or highly excited nuclei is of prime importance both experimentally and theoretically. The experimental study is based upon the fission type or heavy ion reactions. The theoretical studies usually assume thermodynamical equilibrium and introduce the partition function and then calculate the relevant quantities like level density, entropy, excitation energy, etc. Such past theoretical investigations [1] used the statistical model employing the spectra of independent particles moving in an average deformed nuclear potential—thereby calculating the energy surface within the Strutinsky [2] method as a function of deformation for various excitations. This approach is not self-consistent in the sense that the deformation is not calculated self-consistently at each temperature/excitation. Therefore, the temperature dependent mean field approach such as temperature dependent Hartree-Fock method with density dependent interaction of Skyrme type [3] (DDHF-T) is then more appropriate. Such a self-consistent DDHF-T calculation also yields [4] the average potential, single particle states and their occupation probabilities, etc., at each temperature. This then enables us to calculate important quantities like excitation energy, entropy, level density parameter, etc. and also to answer the question *at what temperature the deformation and/ shell effects disappear*. The results of the DDHF-T calculations with the Skyrme-III interaction using a finite basis (oscillator) expansion method reveal [4] that the deformation and the shell effects disappear with increasing excitations, e.g., at around $T\sim 3$ MeV for ^{168}Yb, where the minima of the free energy occurs at zero quadrupole moment/deformation. On the other hand the Strutinsky-type calculation yields zero deformation in general at lower temperatures, e.g., $T\sim 1.8$ MeV for ^{168}Yb. We show here that this difference in the value of temperature T perhaps is due to the value of the effective mass $<$ the free nucleon mass appearing in the Skyrme-III interaction.

The relativistic mean field (RMF) [5,6] has been shown to be very successful for the description of a variety of nuclear properties even for those where the conventional non-relativistic DDHF description was deficient [6]. Therefore, it is worthwhile to extend RMF to include temperature resulting in the temperature dependent RMF (RMF-T), the relativistic counterpart of DDHF-T, and to carry out explicit numerical calculations. Here, we present and discuss some of our temperature dependent relativistic mean field (RMF-T) results for a few selected representative spherical [^{208}Pb, ^{298}GG ($Z=114$)] and deformed (^{168}Er, ^{168}Yb, ^{150}Sm) nuclei, with the following objectives: To demonstrate the feasibility of carrying out such calculations in practice; to bring out the salient general features; and to compare these with the corresponding temperature dependent Hartree Fock (DDHF-T) results obtained with the density dependent interaction of the Skyrme type.

The essential RMF-T equations are presented in Sec. II. Section III contains the details of the calculation. The results are presented and analyzed in Sec. IV. The last section contains the summary and the conclusion.

II. FORMULATION

The conventional temperature dependent Hartree-Fock (HF-T) equations derived by the minimization of the thermodynamical potential have been presented and discussed at various places [4,5]. These HF-T equations retain the same form as that of the Hartree-Fock (HF) [7,8]/RMF equations [6] for the static case. Therefore, here we list the RMF-T equations and introduce the relevant quantities of interest without going into the details. In this mean field variational approach the temperature dependent equations are derived by the minimization of the thermodynamical potential Ω:

$$\Omega = E - TS - \mu N. \tag{1}$$

Here E being the energy, T is the thermodynamic temperature which is introduced through the statistical Fermi occupation probabilities n_i:

$$n_i = \left[1 + \exp\left(\frac{\varepsilon_i - \mu}{kT}\right)\right]^{-1}, \tag{2}$$

for a single particle (sp) orbit $|i\rangle$ having energy ε_i, μ denotes the chemical potential, k the Boltzmann constant and N the particle number. The entropy S is obtained through

$$S = -\sum_i \left[n_i \ln n_i + (1-n_i)\ln(1-n_i)\right]. \tag{3}$$

The minimization of Ω yields the temperature dependent mean field equations:

$$h\phi_i = \varepsilon_i \phi_i, \tag{4}$$

along with the constraint

$$\sum_i n_i = N. \tag{5}$$

Here h denotes the mean field Hamiltonian and the particle number N is the sum of neutrons (N_n) and protons (N_p) and accordingly in Eq. (1)

$$\mu N = \mu_p N_p + \mu_n N_n, \tag{6}$$

with μ_p (μ_n) denoting the chemical potential for protons (neutrons). The one body mean field equations (4) and (5) are similar to the HF equations [7] for the static case and therefore can be solved self-consistently for a given T following the same procedure as adopted for the conventional static HF case. This therefore leads to the self-consistent calculation of the average potential, single particle orbitals and energies ε_i, occupation numbers n_i, density, total energy E, etc. for each temperature T. Using n_i the entropy S can be obtained through [Eq. (3)] and the excitation energy E^* is given by

$$E^*(T) = E(T) - E(T=0), \tag{7}$$

$E(T=0)$ being the energy at zero temperature (ground state). It is to be pointed out that the pairing correlations which are to be included for the correct description of open shell nuclei, are in fact important only at low temperatures ($T<1$ MeV). Therefore, the pairing is taken into account in the constant gap approximation [6,9], only for $T=0$ case and is ignored for $T>0$, i.e., for high excitations.

In the RMF approach one starts with the Lagrangian describing the nucleons interacting with various meson fields. The equations of motion are obtained by using the classical variational principle. Within the mean field approximation which amounts to treating the field operators as c numbers or classical fields, one then ends up with a Dirac equation having Lorentz scalar and vector (fourth component) potentials for nucleons and Klein-Gordon type equations for the meson fields having sources involving various baryon densities. This set of equations are to be solved self-consistently yielding quantities like single particle (sp) potentials, energies, occupation numbers, densities etc.

We consider here the nucleon (Dirac spinor) of mass M interacting with the following meson fields in addition to the electromagnetic field A^μ: The scalar field σ describing the σ meson of mass m_σ with coupling constant g_σ; the vector field ω describing the ω meson of mass m_ω with coupling constant g_ω; and the isovector vector field ρ describing the ρ meson of mass m_ρ with coupling constant g_ρ.

The Lagrangian density for this case is taken to be

$$\begin{aligned}\mathcal{L} = {} & \bar{\psi}_i\{i\gamma^\mu\partial_\mu - M\} + \frac{1}{2}\partial^\mu\sigma\partial_\mu\sigma - U(\sigma) - g_\sigma\bar{\psi}_i\psi_i\sigma \\ & - \frac{1}{4}\Omega^{\mu\nu}\Omega_{\mu\nu} + \frac{1}{2}m_\omega^2\omega^\mu\omega_n u - g_\omega\bar{\psi}_i\gamma^\mu\psi_i\omega_\mu - \frac{1}{4}\mathbf{R}^{\mu\nu}\mathbf{R}_{\mu\nu} \\ & + \frac{1}{2}m_\rho^2\rho^\mu\rho_\mu - g_\rho\bar{\psi}_i\gamma^\mu\tau\psi_i\rho_\mu - \frac{1}{4}\mathbf{R}^{\mu\nu}\mathbf{R}_{\mu\nu} \\ & - e\bar{\psi}_i\gamma^\mu\frac{\mu(1-\tau_z)}{2}\psi_i A_\mu.\end{aligned} \tag{8}$$

The sigma meson is subjected to an additional nonlinear potential,

$$U(\sigma) = \frac{1}{2}m_\sigma\sigma^2 + \frac{1}{3}g_2\sigma^3 + \frac{1}{4}g_3\sigma^4. \tag{9}$$

The symbols $F^{\mu\nu}$ and $\Omega^{\mu\nu}$ ($\mathbf{R}^{\mu\nu}$) denote the field tensors for the electromagnetic and the vector (isovector) meson fields.

Employing the mean field approximation and ignoring the antiparticle (holes in the Dirac sea) contributions to the source terms of the meson fields, for the static spherical case one ends up with the following set of equations.

A coupled set of equations for the large $[f(i)]$ and small $[g(i)]$ components of the Dirac spinor:

$$[M^*(r) + V(r)]f_i(r) + \left(\partial_r - \frac{\kappa_i - 1}{r}\right)g_i(r) = \varepsilon_i f_i(r), \tag{10}$$

$$-\left(\partial_r + \frac{\kappa_i + 1}{r}\right)f_i(r) - [M^*(r) - V(r)]g_i(r) = \varepsilon_i g_i(r), \tag{11}$$

where

$$\kappa_i = \pm\left(j_i + \frac{1}{2}\right) \quad \text{for } j_i = \ell_i \mp \frac{1}{2}$$

and

$$M^*(r) = M + g_\sigma\sigma(r), \tag{12}$$

$$V(r) = g_\omega\omega^0(r) + g_\rho\vec{\tau}\vec{\rho}^0(r) + e\frac{(1+\tau_3)}{2}A^0(r). \tag{13}$$

Klein-Gordon equation:

$$\left(-\frac{\partial^2}{\partial r^2} - \frac{2}{r}\frac{\partial}{\partial r} + m_\phi^2\right)\phi(r) = s_\phi(r). \tag{14}$$

m_ϕ denotes the meson mass for $\phi = \sigma$, ω and ρ and is zero for the photon.

The source term

$$s_\phi(r) = \begin{cases} -g_\sigma \rho_s(r) - g_2\sigma^2(r) - g_3\sigma^3(r) & \text{for the } \sigma \text{ field,} \\ g_\omega \rho_v(r) & \text{for the} \omega \text{ field,} \\ g_\rho \rho_3(r) & \text{for the } \rho \text{ field,} \\ e\rho_p(r) & \text{for the Coulomb field.} \end{cases} \tag{15}$$

The various baryon densities appearing in the source term [Eq. (15)] are given by

$$\rho_s(r) = \sum_i n_i(2j_i+1)(|f_i(r)|^2 - |g_i(r)|^2), \tag{16}$$

$$\rho_v(r) = \sum_i n_i(2j_i+1)(|f_i(r)|^2 + |g_i(r)|^2), \tag{17}$$

$$\rho_3(r) = \sum_i n_i 2t_i(2j_i+1)(|f_i(r)|^2 + |g_i(r)|^2), \tag{18}$$

$$\rho_c(r) = \sum_i n_i\left(\frac{1}{2} - t_i\right)(2j_i+1)(|f_i(r)|^2 + |g_i(r)|^2). \tag{19}$$

The quantities n_i are the occupation numbers. In the simple case with no pairing (magic nuclei) at $T=0$

$$n_i = \begin{cases} 1 & \text{for the occupied levels,} \\ 0 & \text{for the unoccupied levels.} \end{cases} \tag{20}$$

For open shell nuclei with pairing the n_i can be obtained in the constant gap approximation as described in Ref. [6]. For high excitations $T>0$, n_i is given by Eq. (2) in which the chemical potential μ is to be replaced by the corresponding Fermi energy. The Fermi energy is obtained through the constraint

$$\sum n_i = \text{number of neutrons/protons.} \tag{21}$$

To incorporate the finite size of the proton, the calculated point proton density is folded with the proton charge distribution of rms-radius 0.8 fermi having a Gaussian shape. This folded density can then be directly compared with the experimental charge density. Similarly, the charge radii r_c obtained from the calculated point proton rms radii through

$$r_c = \sqrt{r_p^2 + 0.64}$$

can be compared with the corresponding experimental value.

III. DETAILS OF THE CALCULATION

The RMF equations for the spherical (deformed) systems, are solved by expanding separately the large $(f(i))$ and the small $(g(i))$ component of the Dirac spinor and so also the Bose (meson and electromagnetic) fields and the various densities in terms of isotropic (anisotropic) harmonic oscillator basis as described in Ref. [6]. The expansion is truncated so as to include for fermions (mesons) all the states having major oscillator quantum number $[N_{F_{\max}}(N_{B_{\max}})]$. We fix the basis parameters: The size: $\hbar\omega = 41A^{-1/3}$, the deformation $\beta = 0$ (close to the experimental value) for spherical (deformed) nuclei and $N_{F_{\max}} = N_{B_{\max}} = 20(14)$ for spherical (deformed) systems, in accordance with our earlier work ([6]). The parameters appearing in the Lagrangian are taken to be the most up to date set NL3 [10].

The parameters of this NL3 set [10] are as follows:

Masses (MeV): $M = 939.0$, $m_\sigma = 508.194$, $m_\omega = 782.501$, $m_\rho = 763.0$.

Coupling constants: $g_\sigma = 10.217$, $g_\omega = 12.868$, $g_\rho = 4.474$, $g_2 = -10.431$ fm^{-1}, and $g_3 = -28.885$.

First a systematic set of self-consistent RMF-T calculations are carried out for spherical nucleus ^{208}Pb and the hypothetical nucleus ^{298}GG ($Z=114$) for temperatures ranging from 0 to 5 MeV. Some of these results, e.g., the mean field potential, effective mass, densities, etc. are presented and discussed in the next section.

Next, RMF-T calculations for deformed nuclei are carried out. In the next section we present and discuss some of our temperature dependent relativistic mean field (RMF-T) results for a few selected representative deformed (^{168}Er, ^{168}Yb, and ^{150}Sm) nuclei. As stated earlier, pairing is included in the constant gap approximation for the ground state ($T=0$) only for these open shell deformed nuclei. The gap parameters for neutrons (protons) Δ_n (Δ_p) required in the calculation of the respective occupation probabilities are extracted from the odd even mass differences obtained from the published [11] mass tables. The calculated values of Δ_n (Δ_p) for ^{168}Er, ^{168}Yb, and ^{150}Sm are 1.034 (1.176), 1.041 (1.165), and 1.079 (1.213) MeV, respectively. Initially the calculations have been carried out with $N_{F_{\max}} = 12$, $N_{B_{\max}} = 20$ for ^{168}Er, then the same have been repeated with $N_{F_{\max}} = 14$, $N_{B_{\max}} = 20$. Practically no change in the calculated results have been noticed, indicating thereby the required convergence. Thus the results with $N_{F_{\max}} = 12$, $N_{B_{\max}} = 20$ may be reasonable and reliable. For the rest of the calculations presented here we therefore, fix $N_{F_{\max}} = 12$, $N_{B_{\max}} = 20$.

Before closing this section we would like to point out that the contribution due to the evaporation of nucleons which

TABLE I. The calculated self-consistent RMF-T total binding energy E, point neutron radius r_n, charge radius r_c, the root mean square radius $r_{\rm rms}$, and the entropy S for the various values of the temperature T obtained by using the Lagrangian parameter set NL3. The experimental ground state ($T=0$) values are give in the parenthesis.

^{208}Pb					
T	E	r_n	r_c	$r_{\rm rms}$	S
0.0	1639.5	5.74	5.52	5.63	
	(1636.5)		(5.50)		
1.0	1626.6	5.75	5.54	5.65	17.70
2.0	1567.7	5.83	5.57	5.70	57.01
3.0	1469.2	5.98	5.61	5.82	96.35
3.5	1401.8	6.09	5.65	5.90	117.07
4.0	1320.4	6.22	5.72	6.00	138.75
^{298}GG($Z=114$)					
0.0	2123.9	6.51	6.26	6.39	
1.0	2100.6	6.52	6.29	6.41	40.95
2.0	2026.1	6.58	6.31	6.46	90.40
3.0	1888.2	6.73	6.35	6.57	145.29
3.5	1789.4	6.84	6.39	6.65	175.64
4.0	1667.6	6.96	6.45	6.75	208.04

starts becoming relevant with increasing temperature, is ignored in the present work. Bonche *et al.* [12] incorporated this contribution in an approximate manner. In the correct description this contribution should be taken into account accurately. However, this problem still awaits a satisfactory solution. Therefore, in the present context our results are reliable for temperatures T up to say 3 MeV, above which uncertainties may start creeping in. Therefore, to be on the conservative side, we present and discuss the rest of our results (i.e., for deformed systems) only for temperatures $T \leqslant 3$ MeV.

IV. RESULTS AND DISCUSSION

First we analyze our self-consistent RMF-T results for the nucleus ^{208}Pb, celebrated representative of spherical nuclei, arranged in Table I. Similar results for a hypothetical superheavy spherical nucleus ^{298}GG ($Z=114$) are also arranged in the same table. The corresponding experimental values for the ground state ($T=0$), where available, are shown (in parentheses). The ground state properties are well reproduced as was found earlier. With the increase in temperature T the higher lying levels start getting partially occupied, resulting in the decrease in binding energy and slight increase in radii. The increase in radii as T increases, is very slow in the beginning and later becomes relatively fast. These features are as expected and are consistent with those found in the corresponding nonrelativistic (DDHF-T) calculations [4] with Skyrme-type interaction. The single particle level energies (ε_i) vary only slightly with temperature. In general the lowest levels very slightly increase with temperature whereas the high-lying levels decrease. The maximum variation is ~ 1.5 MeV for temperatures between $T=0-5$ MeV. This observation holds true both for proton and neutron levels. To understand this remarkable constancy of ε_i we examine the variation of the calculated effective mass, local potentials and the density distributions. This is because these quantities are interlinked in this self-consistent mean field approach. These are shown in Figs. 1–4, respectively. The calculated proton local potential (Fig. 1) oscillates in the interior. The magnitude of oscillation decrease with the increase in temperature. This oscillatory behavior is purely a manifestation of coulomb effect and is therefore absent in the neutron potential (Fig. 1). The potential increases (less attractive) and vanish at the surface but at a slightly larger radius as the temperature rises, both for neutrons and protons. This feature

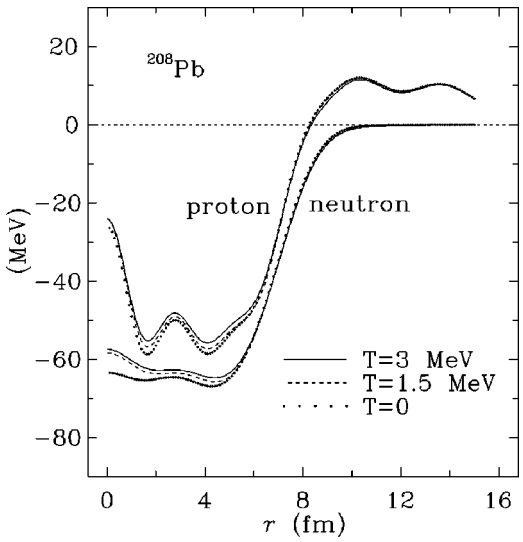

FIG. 1. The calculated RMF-T effective potential as a function of the radial distance r for protons and neutrons for the spherical nucleus ^{208}Pb at temperatures $T=0$, 1.5, and 3.0 MeV.

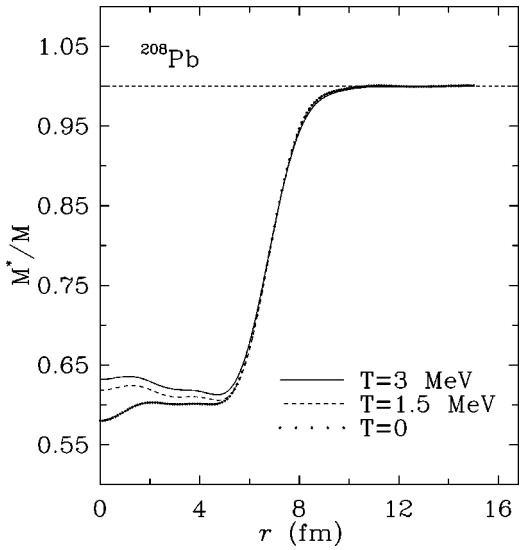

FIG. 2. The calculated RMF-T ratio (M^*/M) of the effective mass to the bare mass as a function of the radial distance r for the spherical nucleus ^{208}Pb at temperatures $T=0$, 1.5, and 3.0 MeV.

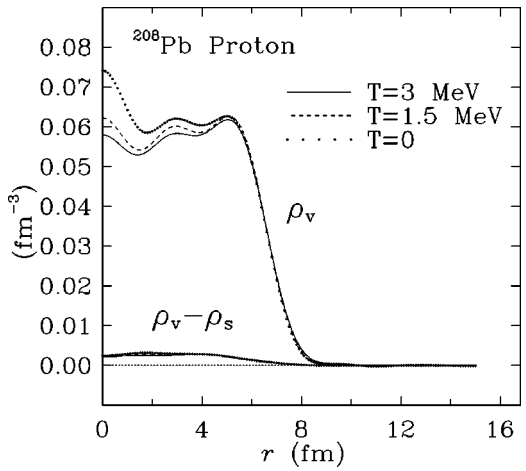

FIG. 3. The calculated RMF-T vector density (ρ_v) and the difference between the vector density and the scalar density $\rho_v-\rho_s$ as a function of the radial distance r for protons in the spherical nucleus ^{208}Pb at temperatures $T=0$, 1.5, and 3.0 MeV.

is expected to directly manifest in the calculated effective mass (Fig. 2). We see that with the increase in temperature the effective mass (Fig. 2) slightly increases in the interior and approaches to the bare value at the surface but at a slightly larger value of r. This behavior of the potentials and the effective mass is directly linked with the decrease in the density in the interior, as is expected. The calculated point proton and neutron densities are shown in Figs. 3 and 4 respectively for various values of temperature T. These show oscillations in the interior which are relatively larger for the point proton densities. These oscillations reduce in magnitude with increase in T and eventually expected to disappear at larger T ($\sim$5 MeV). Thus the heating of the system results in smoothening of the oscillations. Further, the central density is clearly lowered (decreases in the interior) and the surface region is broadened (extends further out) with increase in T, resulting an increase in the rms radii. This is expected as with the heating of the system more and more high lying levels start getting partially occupied.

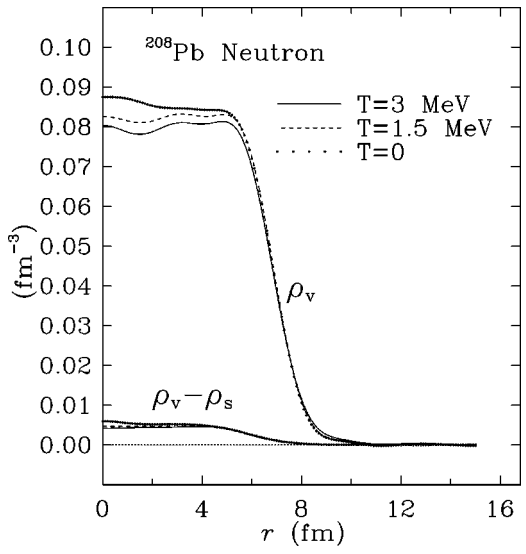

FIG. 4. The calculated RMF-T vector density (ρ_v) and the difference between the vector density and the scalar density $\rho_v-\rho_s$ as a function of the radial distance r for protons in the spherical nucleus ^{208}Pb at temperatures $T=0$, 1.5, and 3.0 MeV.

Now we consider the effect of these variations on the single particle spectrum: An increase in the effective mass raises the deep lying levels but lowers the high lying levels. On the other hand, an increase in the radius lowers the entire spectrum. Thus these two effects cancel in the lower part of the spectrum while they go in the same direction for the high lying states. The net effect is that the lowest levels increase very slightly with T whereas high lying levels decrease. Overall there is only a small variation in the single particle level spectrum.

For deformed systems we expect more changes in the average field with the increase in temperature T. This is because the melting of shell effects at higher excitations will make the nucleus spherical. Therefore, we next analyze the representative results of deformed nuclei. We select ^{168}Er and ^{168}Yb, both are well studied and are well deformed systems. The calculated RMF-T results for various temperatures T are arranged in Table II against the label NL3. Clearly, the calculated ground state ($T=0$) total binding energy, charge radius r_c and the deformation β compare very well with the corresponding experimental values (given in parentheses), as found in earlier studies. The total binding energy E decreases while the entropy S increases as T increases. The deformation β (so also the quadrupole moment q_2 and hexadecupole moment h_4) slowly decrease with the rise in temperature T. At temperature close to $T\sim3$ MeV the deformation vanishes and the nucleus becomes spherical. The charge and the rms radii are minimum at this temperature corresponding to the spherical shape. Beyond this critical temperature ($T\sim3$ MeV) the calculated E (S) decrease (increase) and the radii increase as T increases similar to that observed for the spherical systems.

We also consider the nucleus ^{150}Sm a relatively less deformed system. Similar observations also hold for the calculated RMF-T results (presented in Table II) for ^{150}Sm. Here the deformation β vanishes at temperature close to 2 MeV, relatively earlier as compared to that for the well deformed nuclei.

The disappearance of shell effects can also be seen by studying the variation of entropy S as a function of excitation energy. At high T which is sufficient to wipe out the shell effects, the entropy S and excitation energy E^* are expected to be related by the asymptotic formulas [13]:

$$S\sim 2\sqrt{a(E^*+\Delta E_0)},$$

$$E^*=aT^2-\Delta E_0. \tag{22}$$

Here ΔE_0 ($\ll E^*$) is the ground state shell correction and a the level density parameter which is related to $\bar{g}(\mu)$ the average density of single particle states ε_i at the Fermi energy, through a factor $\pi^2/6$.

One can check these asymptotic relations by examining

TABLE II. The calculated self-consistent RMF-T results (marked NL3): total binding energy E, point neutron radius r_n, charge radius r_c, the root mean square radius $r_{\rm rms}$, the deformation β, the quadrupole moment q_2, hexadecupole moment h_4, the entropy S and $S/2T$ for the various values of the temperature T for deformed representative nuclei. The experimental ground state ($T=0$) values are give in the parenthesis. The corresponding DDHF results with Skyrme (SK-III and SKP) interactions are also listed.

^{168}Er										
T		E	r_n	r_c	$r_{\rm rms}$	β	q_2	h_4	S	$S/2T$
0.0	NL3	1365.6	5.45	5.28	5.36	0.35	19.3	0.67		
	SK-III	1358.9	5.41	5.37	5.37	0.36	19.9	0.90		
	SKP	1361.6	5.38	5.32	5.33	0.35	19.4	0.71		
	Expt.	(1365.8)		(5.31)		(0.34)				
1.0	NL3	1352.4	5.44	5.28	5.35	0.33	18.5	0.63	21.99	10.99
	SK-III	1332.3	5.39	5.35	5.35	0.34	18.8	0.76	24.48	12.24
	SKP	1338.0	5.36	5.29	5.31	0.32	17.9	0.61	32.59	16.30
2.0	NL3	1309.3	5.43	5.25	5.34	0.23	12.8	0.28	50.50	12.63
	SK-III	1278.9	5.36	5.30	5.31	0.20	10.9	0.22	55.54	13.89
	SKP	1282.8	5.31	5.22	5.25	0.07	4.1	0.04	69.08	17.27
3.0	NL3	1245.2	5.45	5.24	5.34	0.00	0.2	0.03	76.39	12.73
	SK-III	1210.4	5.38	5.29	5.32	0.06	3.5	0.04	85.01	14.17
	SKP	1204.4	5.38	5.26	5.31	0.05	2.6	0.05	103.76	17.29
3.5	NL3	1208.3	5.48	5.25	5.36	0.01	2.3	0.02	87.74	12.53
	SK-III	1168.2	5.42	5.30	5.35	0.06	3.1	0.04	100.61	14.37
^{168}Yb										
0.0	NL3	1363.4	5.41	5.29	5.33	0.32	17.8	0.75		
	SK-III	1357.9	5.40	5.38	5.37	0.35	19.3	0.99		
	SKP	1361.5	5.36	5.33	5.33	0.34	18.9	0.74		
	Expt.	(1362.8)		(5.28)		(0.33)				
1.0	NL3	1349.9	5.40	5.29	5.33	0.31	17.4	0.64	22.73	11.36
	SK-III	1329.7	5.38	5.36	5.34	0.32	18.0	0.78	25.34	12.67
	SKP	1334.0	5.34	5.30	5.29	0.30	16.6	0.55	33.27	16.64
2.0	NL3	1308.5	5.40	5.26	5.32	0.21	11.7	0.25	50.08	12.52
	SK-III	1277.2	5.34	5.31	5.30	0.17	9.7	0.18	55.45	13.86
	SKP	1282.8	5.30	5.24	5.25	0.07	3.7	0.04	68.43	17.11
3.0	NL3	1246.0	5.41	5.26	5.32	0.07	3.9	0.04	75.25	12.54
	SK-III	1211.6	5.36	5.31	5.31	0.06	3.6	0.04	84.36	14.09
	SKP	1205.9	5.35	5.29	5.30	0.05	2.8	0.06	103.22	17.24
3.5	NL3	1208.7	5.44	5.27	5.35	0.06	3.2	0.03	86.76	12.39
	SK-III	1171.0	5.39	5.33	5.34	0.06	3.4	0.05	100.01	14.29
^{150}Sm										
0.0	NL3	1239.3	5.19	5.05	5.10	0.20	9.2	0.60		
	SK-III	1226.6	5.16	5.14	5.12	0.22	10.2	0.67		
	SKP	1236.3	5.11	5.06	5.07	0.16	7.2	0.13		
	Expt.	(1236.2)		(5.05)		(0.19)				
1.0	NL3	1226.0	5.18	5.04	5.10	0.19	8.6	0.48	21.70	10.85
	SK-III	1201.1	5.14	5.11	5.11	0.20	9.3	0.50	24.86	12.43
	SKP	1211.6	5.10	5.04	5.05	0.13	6.1	0.11	31.19	15.60
1.5	NL3	1210.5	5.17	5.03	5.09	0.11	5.0	0.16	34.11	11.37
	SK-III	1182.0	5.13	5.09	5.09	0.11	5.1	0.13	37.79	12.60
	SKP	1193.1	5.10	5.03	5.04	0.04	1.9	0.02	46.10	15.37
2.0	NL3	1190.8	5.18	5.02	5.09	−0.02	−0.7	−0.02	45.41	11.36
	SK-III	1161.2	5.13	5.09	5.09	0.03	1.6	0.01	49.84	12.46
	SKP	1168.0	5.11	5.05	5.06	0.02	1.1	0.01	61.09	15.29

$$\frac{1}{4}\left(\frac{dS^2}{dE^*}\right)=\frac{S}{2T}$$

and

$$\frac{dE^*}{dT^2},$$

which can be evaluated numerically from the finite differences obtained at different temperatures. We include some of these results in Table II. The tables show that $S/2T$ approaches almost a constant value close to the temperature where the deformation vanishes (disappearance of shell effects). This holds for the results of all the three deformed cases, listed in the tables.

The corresponding DDHF-T results with Skyrme III interaction for ^{168}Er, ^{168}Yb, and ^{150}Sm are also listed in Table II against the label SK-III. These SK-III results show identical trends as those observed for the respective RMF-T results. It is now known that fully self-consistent mean field calculations like the DDHF-T with the Skyrme-III interaction or RMF-T reveal that the deformation and the shell effects disappear with increasing excitations at around $T\sim 3$ MeV for well deformed nuclei like ^{168}Yb. On the other hand the Strutinsky-type calculation yields zero deformation, in general, at lower temperatures, e.g., $T\sim 1.8$ MeV for ^{168}Yb. This difference in the value of temperature T may be either due to the lack of self-consistency in the Strutinsky-type calculations and/or due to the use of the value of the nucleon effective mass [$M^*<$ the bare mass (M)] appearing in Skyrme-III interaction or resulting from the RMF Lagrangian. To examine the problem of the self-consistency we first carried out the self-consistent RMF calculations for different deformations β generating energy (E) versus deformation (β) curve for the ground state ($T=0$) of ^{168}Er. It is observed that the lowest energy (maximum binding) occurs at the β value equal to that listed in Table II for $T=0$. Then we carried out the self-consistent RMF-T constraint (on the deformation β: fixed to the ground state value) calculations for various temperatures (T). It is observed that this constraint does not change the total energy E and so also the single particle energies (ε_i). These observations then indicate that the lack of self-consistency is not the origin of the difference in the value of temperature T where the deformation and shell-effects disappear, obtained in the self-consistent mean field approach and the Strutinsky approach. Therefore, we then considered the problem related to the effective mass and repeated the self-consistent DDHF-T calculations using the Skyrme interaction SKP [14] and the same values of the pairing gaps Δ_n and Δ_p as before. These results for ^{168}Er, ^{168}Yb, and ^{150}Sm are also listed in Table II. The interaction SKP has the effective mass (M^*) equal to the bare mass (M). The ground state DDHF-T results with SKP interaction are almost identical to those of SK-III, as expected because that was the criterion used in generating these SK-III and SKP interaction parameters. The calculations reveal that the deformation (β) now disappears at lower temperature ($T\sim 2$ MeV) for both ^{168}Er and ^{168}Yb. This value is very close to that obtained in the Strutinsky calculation for these nuclei.

The DDHF-T results with SKP interaction for ^{150}Sm indicate that the temperature T where the deformation β disappears is ~ 1.5 MeV, slightly lower as compared to that for well deformed systems (e.g., ^{168}Er and ^{168}Yb). This value (1.5 MeV) is also close to the value expected from the Strutinsky approximation.

Based on this analysis, one may therefore, conclude that the above mentioned difference in the value of the temperature (T) where the shell effects disappear in the self-consistent mean field approach and the Strutinsky approach, is due to the use of the value of the effective mass less than the bare mass in the former.

V. SUMMARY AND CONCLUSION

We have carried out self-consistent temperature dependent relativistic mean field (RMF-T) calculations for some sample spherical and deformed nuclei, demonstrating thereby the feasibility of carrying out such temperature dependent calculations in practice. The analysis of the results reveal systematics very similar to those observed in the corresponding nonrelativistic temperature dependent Hartree-Fock (DDHF-T) studies with density dependent Skyrme-type interactions (SK-III and SKP). The energy decreases (less negative) while the size (radii) increases as temperature increases. The deformed systems tend to become spherical as temperature rises. Shell effects wash out at high excitations, i.e., with rising temperatures (T). The melting away of shell effects for well deformed nuclei is at temperature $T\sim 3$ MeV while it is at a lower temperature (around $T\sim 2$ MeV) for moderately deformed systems. The Strutinsky calculations yield relatively less value of the temperature (T) at which the deformation vanishes ($\beta\rightarrow 0$) as compared to that obtained in the self-consistent mean field approaches like DDHF-T with Skyrme III (SK-III) interaction or RMF-T. On the other hand the DDHF-T results (SKP) with Skyrme Interaction SKP (having effective nucleon mass the same as the bare mass) yield this value of temperature T close to the value obtained in the Strutinsky type calculations. This difference in the value of the temperature is therefore, expected to be due to the lower value ($<$ the bare mass) of the nucleon effective mass resulting in the SK-III interaction or from the RMF Lagrangian.

[1] M. Brac, J. Damgaard, A. S. Jensen, H. C. Pauli, V. M. Strutinsky, and C. Y. Wong, Rev. Mod. Phys. **44**, 320 (1972).
[2] V. M. Strutinsky, Nucl. Phys. **A95**, 420 (1967); **A122**, 1 (1968).
[3] T. H. R. Skyrme, Philos. Mag. **1**, 1043 (1956).
[4] M. Brac and P. Quentin, Phys. Lett. **52B**, 159 (1974); Phys. Scr. **10**, 163 (1974).
[5] B. D. Serot and J. D. Walecka, Adv. Nucl. Phys. **16**, 1 (1986);

C. J. Horowitz and B. D. Serot, Nucl. Phys. **A386**, 503 (1981); Suk-Jean Le *et al.*, Phys. Rev. Lett. **57**, 2916 (1986); B. D. Serot, Rep. Prog. Phys. **55**, 1855 (1992); P. G. Reinhard, *ibid.* **52**, 439 (1989); P. Ring, Prog. Part. Nucl. Phys. **37**, 193 (1996).

[6] Y. K. Gambhir, P. Ring, and A. Thimet, Ann. Phys. (N.Y.) **198**, 132 (1990), and references cited therein; J. P. Maharana, Latha S. Warrier, and Y. K. Gambhir, *ibid.* **250**, 237 (1996); P. Ring, Y. K. Gambhir, and G. A. Lalazissis, Comput. Phys. Commun. **105**, 77 (1997).

[7] D. Vautherin and D. M. Brink, Phys. Rev. C **5**, 626 (1972); D. Vautherin, *ibid.* **7**, 296 (1973).

[8] J. Friedrich and P. G. Reinhard, Phys. Rev. C **33**, 335 (1986).

[9] P. Ring and P. Schuck, *Nuclear Many Body Problem* (Springer-Verlag, Heidelberg, 1980).

[10] G. A. Lalazissis, J. König, and P. Ring; Phys. Rev. C **55**, 540 (1997).

[11] G. Audi and A. H. Wapstra, Nucl. Phys. **A565**, 1 (1993); **A565**, 66 (1993).

[12] P. Bonche, S. Levit, and D. Vautherin, Nucl. Phys. **A427**, 278 (1984).

[13] V. S. Ramamurthy, S. S. Kapoor, and S. K. Kattaria, Phys. Rev. Lett. **25**, 386 (1970); J. R. Huizenga and L. G. Moretto, Annu. Rev. Nucl. Sci. **22**, 427 (1972).

[14] J. Dobaczewski *et al.*, Nucl. Phys. **A422**, 103 (1984).